Digest Journal of Nanomaterials and Biostructures Vol. 9, No. 4, October - December 2014, p. 1451 - 1459

IONIC LIQUID ASSISTED THE PREPARATION OF ANATASE TiO_2 WITH HIGH SURFACE AREA AND POROUS STRUCTURE

D. SUN, C. YU, G. SHAO, H. DAI, X. DONG, Y. MA*
School of Light Industry & Chemistry Engineering, Dalian Polytechnic University, Dalian 116034, China

The porous anatase TiO_2 with high surface area and uniform pore structure were synthesized at low temperature and ambient pressure with tetrabutyl titanate as precursor, ionic liquid [C_6mim]Br as template. The obtained materials were characterized by Fourier transform (FT-IR) spectra, energy dispersive X-ray (EDX) spectroscopy, powder X-ray diffraction (XRD), Brunauer-Emmett-Teller (BET), scanning electron microscopy (SEM) and transmission electron micrographs (TEM). The results showed that the ionic liquid [C_6mim]Br, as a effective template, encouraged the formation of anatase crystal by sol-gel method, meanwhile the anatase TiO_2 formed high surface area and porous structure. Furthermore, it enhanced the photocatalytic activity in the degradation of reactive brilliant blue KN-R (RBB).

(Received September 13, 2014; Accepted November 3, 2014)

Keywords: TiO_2 · Ionic liquid · Porous structure · Photocatalytic activity

1. Introduction

Titanium oxide (TiO_2) has attracted great attention for its wide application, such as being photocatalyst, catalyst support, photovoltaic solar cell, gas sensor, etc. The application and properties of TiO_2 depended on its own crystalline phase, conformation and particle size [1]. Recently, fabrication of nanostructured TiO_2 with small grain size, high specific surface area, controlled porosity and tailor-designed pore size distribution have been widely studied. However, in order to overcome the low recuperability of TiO_2 powder in application, it was highly desirable to synthesize TiO_2. In previous studies, TiO_2 were prepared in common with using supercritical drying and needing a high temperature heat treatment for crystallization. These processes can lead to fragility of the products and reduction of its specific surface area [2]. Therefore, it was significant to prepare stable and crystalline TiO_2 nanostructures at low temperature and ambient pressure, and this goal can be achieved by the assist of ionic liquid.

Ionic liquid (IL), it is entirely composed of ions and has many advantages, low melting point, high boiling point, low vapor pressure, good thermal stability and chemical stability, it's widely used in organic synthesis, separation and other fields, but the study on synthesis of porous materials is still in the initial stage. Using IL as the template agent in the synthesis of porous materials opens up a new way for preparing porous materials, especially, it is in line with the requirements of green chemistry and full of study value [3]. In recent years, scientists have used IL to assist the synthesis of porous TiO_2.

In previous studies, Yu [4] prepared TiO_2 photocatalyst in ionic liquid [C_4mim]BF_4, enhanced its response to visible light. Zheng [5] prepared rutile and anatase rutile − composite phase TiO_2 nanoparticles by hydrolysis of $TiCl_4$ in the mixed solution of ionic liquids [C_2mim]Br and hydrochloric acid. Liu Hong [1] has produced anatase structured TiO_2 nano particles at the

* Corresponding author: z19811229@126.com

temperature 60 ℃ - 100 ℃ with hot method and state the effect of the ionic liquid [Bmim]BF_4. Yoo [6, 7] has also synthetized anatase structured TiO_2 nano particles in the ionic liquid [Bmim]BF_4 at room temperature with the sol-gel method.

But there are two obvious drawbacks of these experiments, first one is the synthetic method which uses heat and pressure, second one is molded samples own defects of small specific surface area, pore collapse and phase instability. So the low temperature and ambient pressure preparation of high crystalline with a large specific surface area have been a subject studied by many workers [8-11]. In our experiments, the TiO_2 were synthesized by a novel sol-gel method, which was to synthesize TiO_2 with tetrabutyl titanate as precursor, ionic liquid [C_6mim]Br as template at low temperature and ambient pressure, without other assistant means like reaction kettle and microwave heat treatment, while the formation of anatase phase is stable and TiO_2 formed high surface area and porous structure.

2. Experimental

2.1 Chemicals

Tetrabutyl titanate ($Ti(OC_4H_9)_4$, TBOT), absolute ethyl alcohol (C_2H_5OH, EtOH) and ethylic acid (CH_3COOH) are all purchased from Beijing Chemical Reagent Company, ionic liquid [C_6mim]Br (IL) is purchased from Lanzhou Institute of Chemical Physics, deionized water.

2.2 Preparation of TiO_2

The preparation of TiO_2 was about Sample A and B, as the table 1 showed. Their ways of preparation are the same, but Sample B was obtained with IL and Sample A was not, so we only introduced Sample B as an example.

The TiO_2 were synthesized with tetrabutyl titanate as precursor, absolute ethyl alcohol as solvent, ionic liquid [C_6mim]Br as catalyst and template. The molar ratio of these chemicals was n(IL) : n(TBOT) : n(EtOH) : n(CH_3COOH) : n(H_2O) = 1.5 : 1 : 21 : 1.8 : 6.

Table 1 The preparation of Sample A and B

Samples	Template	Aging liquid
A	Nothing	Water
B	IL	Water solution of IL

According to the above proportion, the EtOH was divided equally into two parts. The TBOT was dissolved into one part of the EtOH firstly, and adding the aqueous solution of ethylic acid, H_2O and IL into the other part of EtOH, then hydrolyzing the two. The TiO_2 sol was obtained under vigorous stirring. And then the TiO_2 alcogels was obtained after standing the TiO_2 sol at room temperature.

The 1.5 mol·L^{-1} IL aging liquid was added to the alcogel for aging it 4 days at 60 ℃, and then the product was dipped in the absolute ethyl alcohol to swap out the remained IL, repeat this five times with each time 4 hours. Dipped the alcogel again with cyclohexane as desiccant, repeated this four times with each time 3 hours, circumfused to desiccate the alcogel fully with the desiccant. The TiO_2 were produced after drying the processed alcogel 24 hours at room temperature and 12 hours at 60 ℃ in the vacuum desiccators.

2.3 Characterization

The Fourier transform spectra was recorded with Nicolet NEXUS 6700 and the energy dispersive X-ray spectroscopy was recorded with Oxford INCA.

The X-ray powder diffraction measurements were performed on a D/Max-3B X-ray diffractometer using SHIMADAZU LabX XRD-6100, Cu-Kα-radiation (λ=1.5406 nm) of 40 kV and 30 mA.

The specific surface area of each sample was calculated by using the BET method. The BET surface areas of the catalysts were measured using JW-BK222 surface area and pore size analyzer (Beijing JWGB Sci.&Tech. Co. Ltd. China).

The sample morphology was observed by the transmission electron micrographs (JEOL, JEM-2100) and the scanning electron micrographs (JEOL, JSM-7001F).

2.4 Photocatalytic activity

The photocatalytic degradation of RBB KN-R was carried out at room temperature by 50 W UV mercury lamp. For these experiments on photocatalytic degradation, the following conditions were that the initial concentration of reactive brilliant blue was prepared at 40 $mg \cdot L^{-1}$ and it was used at 400 ml, then the prepared TiO_2 was injected into it at 0.1 g. After stirring in the dark without UV radiation for 60 min to fully adsorb the reactive brilliant blue on the TiO_2 particles, the photocatalytic reaction was initiated by irradiating with UV mercury lamp for 120 min. The absorbance of the samples were checked through UV-Vis, MAPADA UV-1600. And the degradation rate percent (R_d) of RBB KN-R was calculated according to the following expression:

$$R_d=(1-A/A_0)\times 100\%$$

in which A_0 was the absorbance of initial water solution of RBB and A was the absorbance of the water solution of RBB which was degraded by TiO_2 after 120 min.

3. Results and discussion

3.1 FT-IR spectra and EDX spectroscopy analysis of TiO_2

Fig.1 showed the FT-IR spectra of IL and Sample B. From the IL's spectra, 2859 cm^{-1}, 2932 cm^{-1} and 3060 cm^{-1} in the Area Ⅰ were the C–H vibration peaks of the alkyl chain of ionic liquid. From the Area Ⅱ, the ring symmetric stretching vibration of [C6mim]Br was observed to shift from 1571 cm^{-1}. Strong and broad peaks occurred in the regions of 1461 cm^{-1} and 1167 cm^{-1} corresponding to the ring stretching and bending vibration of [C6mim]Br. Opposite to the IL, the spectra of Sample B showed more subdued characteristic peaks of IL in the Area Ⅰ and Ⅱ, meanwhile they occurred to shift because of the π–π stacking interaction existed between the imidazolium rings of [C6mim]Br [9]. But it was obvious that the peak of 656 cm^{-1} was the absorption peak of the Ti–O. This indicated that TiO_2 has been prepared by this method and the IL can be also almost largely swapped out with absolute ethyl alcohol and IL-aging liquid from the TiO_2.

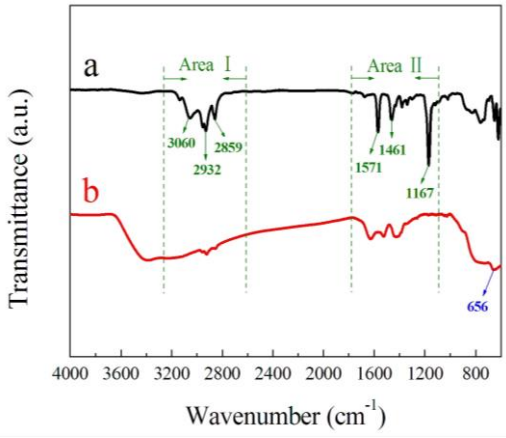

Fig.1 The FT-IR spectra of (a) IL and (b) Sample B

Meanwhile, the Fig.2 also showed that IL-aging liquid and ethyl alcohol can swap out the IL in TiO_2 almost totally, because of the nitrogen element in the imidazole ring of the IL wasn't obviously showed in the EDX spectroscopies. So this indicated that it is an useful method to wipe out the template without other extracting agent which loose amount of reagent and the IL achieved a large proportion of reclamation by our preparation method.

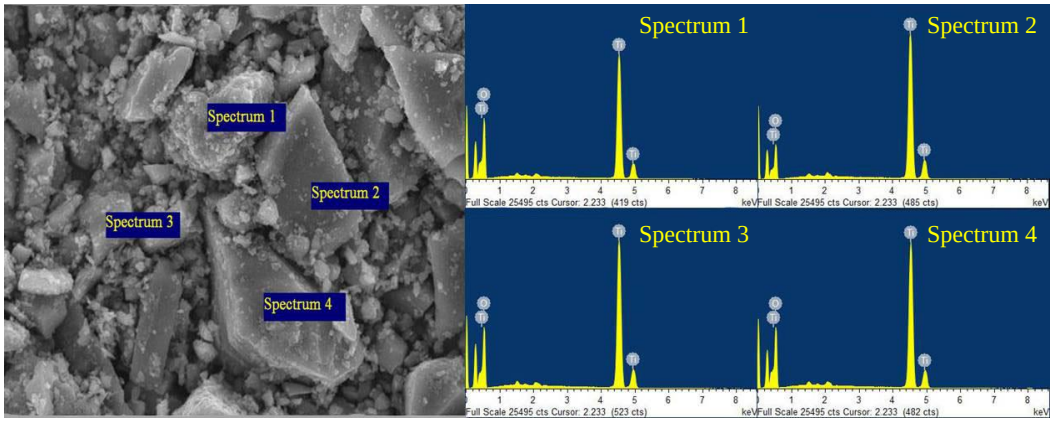

Fig.2 The EDX spectroscopy of different positions of Sample B

3.2 Crystal analysis of TiO_2

XRD patterns of TiO_2 prepared at different conditions were showed in Fig.3. It was observed that the Sample A showed amorphous structure, whereas the peaks of the Sample B were indexed as (101), (004), (200), (105), (204), (215) which assigned to anatase TiO_2 [12]. Meanwhile the Sample B also had no indications of other phases although it was dried at low temperature, 60 ℃. This indicated that IL and IL-aging liquid encouraged the formation of anatase TiO_2.

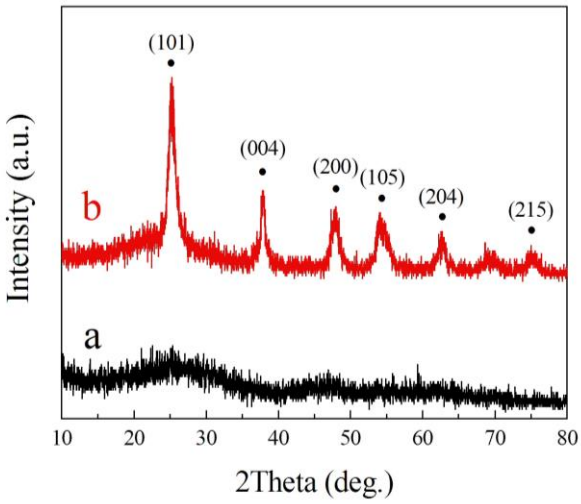

Fig.3 XRD patterns of (a) Sample A and (b) Sample B

The average crystal size of the Sample B was 8.72 nm calculated by using the Scherrer equation based on the XRD peak broadening analysis at the (101) peak [13],

$$D_{hkl}=K\lambda/\beta_{hkl}\times\cos\theta_{hkl}$$

in which D_{hkl} is the crystallite size, λ is the wavelength of incident ray, β_{hkl} is the full width at half-maximum of the peak, and θ is the position of plane peak.

3.3 Specific surface area and pore size distribution of TiO_2

The N_2 adsorption-desorption isotherm and pore size distribution of samples were illustrated in Fig.4. The isotherm pattern of Sample A exhibited type I-like isotherm, this was the characteristic of the narrow pore adsorption, it was caused by the gap between the particles, it was also confirmed that the particles formed reunion without vesicular structure [14]. The Sample B exhibited type IV-like isotherm with H2-like hysteresis loop, which were characteristics of vesicular materials based on the IUPAC classification. And the average pore diameter of the Sample B mainly focuses on 7.605 nm, the vesicular size. The BET surface area and specific pore volume of the material were about 309.769 $m^2\cdot g^{-1}$ and 0.537 $cm^3\cdot g^{-1}$, respectively. However, the pore diameter of Sample A spread unwell-distribute, the BET surface area and specific pore volume were only 43.853 $m^2\cdot g^{-1}$ and 0.161 $cm^3\cdot g^{-1}$.

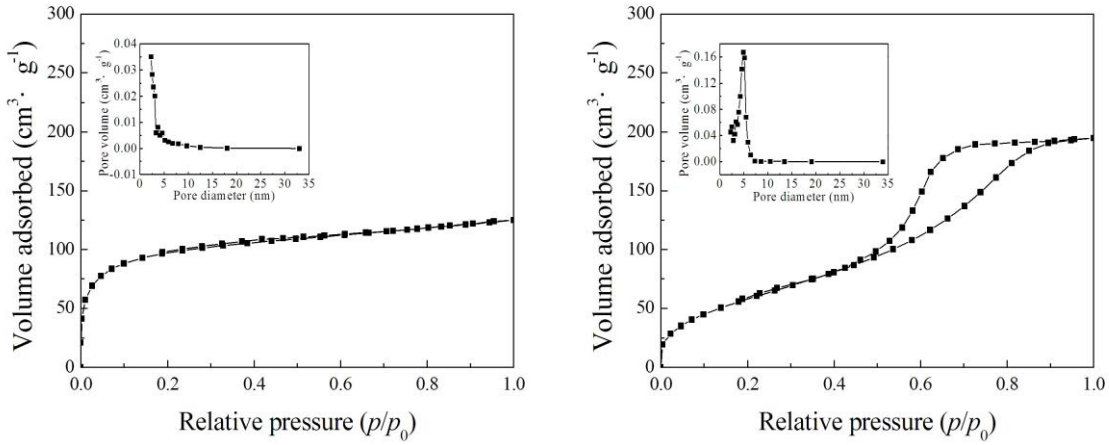

Fig.4 N_2 adsorption-desorption isotherms and pore size distribution curves of (a) Sample A and (b) Sample B

Zhou [15] and co-workers pretreated porous silica with wormhole framework with $[C_4mim]BF_4$ as template. This study proposed a hydrogen bond-co-π–π stack mechanism. The hydrogen bonds formed between the $[BF_4]^-$ and silano group of silica gel and the π–π stack interaction of the neighboring imidazolium rings both play crucial roles in the formation of the wormhole framework of porous silica. In our work, the results of the N_2 adsorption-desorption isotherm and pore size distribution also showed that IL as the template, promoted the formation of high surface area and porous structure of TiO_2.

3.4 Morphology analysis of TiO_2

The SEM images of the Sample A and B were showed in Fig.5. As can be seen clearly in the image a, the Sample A formed reunion with uneven TiO_2 particles, it had no obvious pore structure. From the image b, the Sample B was composed of the relatively uniform porous structure, formed a three-dimensional shape, this indicated that IL promoted the formation of vesicular structure as template.

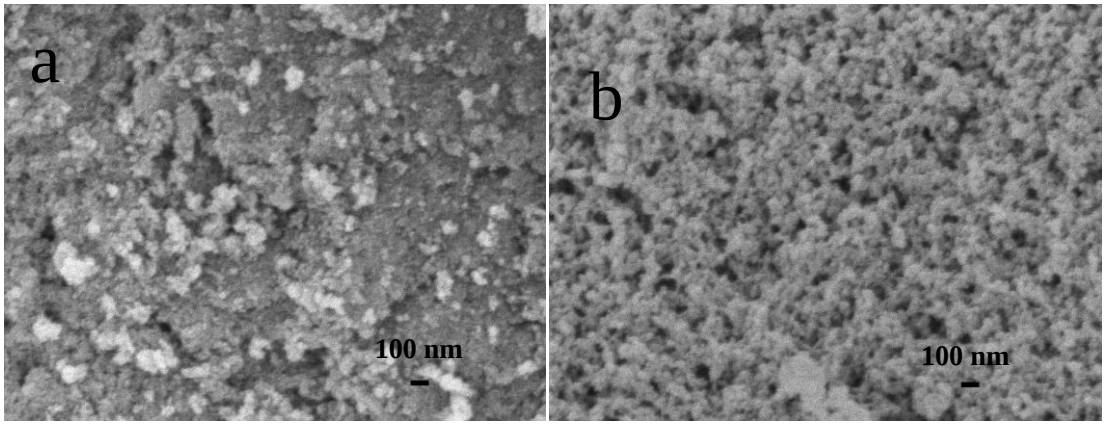

Fig.5 The SEM images of (a) Sample A and (b) Sample B

And, the image a in Fig.6 showed that the Sample B was made up of obviously rodlike-structure minute crystals and owned clear vesicular structure. These indicated that the Sample B has been polycrystalline structure [16]. The sizes of the primary particles were about 9 nm, which was in agreement with the XRD result. The image b showed that the Sample B owned clear crystal lattice, in the HRTEM image, the fringe spacing of 0.308 nm can be indexed to the (101) plane of anatase TiO_2.

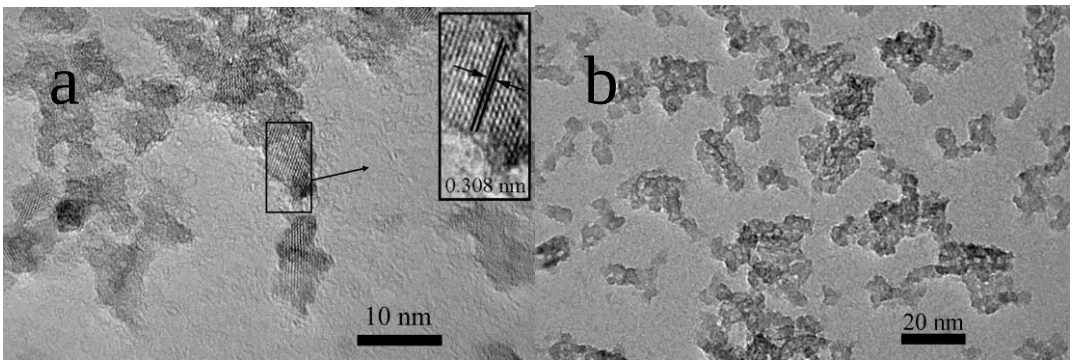

Fig.6 The TEM images (a) and (b) both of Sample B

From metal alkoxide to the formation of metal oxide, there are two processes: hydrolysis and polycondensation. Titanic alkoxide reacts with water under an acidic medium, the titanium ion forms an octahedral structure of $Ti(OH)_m(H_2O)_{6-m}^{(m-4)-}$ [17, 18]. Then, the structures dehydrate each other and polycondensed into the final precipitate [19-21]. It has been proposed that the SO_4^{2-} would influence the formation mechanism of anatase. Because of the steric effect of SO_4^{2-}, the octahedron is more conducive to the formation of an anatase nucleus. The more SO_4^{2-} there are, the more anatase nuclei can be formed. The TiO_2 clusters grow further on the nucleus and then form the anatase phase. It has been reported that the presence of SO_4^{2-} accelerated the growth of TiO_2 clusters to anatase. In our work, $[C_6mim]Br$ promoted the formation of anatase crystal. $[C_6mim]Br$ is composed of the imidazolium cation and Br^- anion, but the radius of SO_4^{2-} (0.245 nm) is much bigger than Br^- (0.196 nm). So we speculated that the imidazolium cation play crucial roles in the steric effect, not only the hydrogen bonds formed between the Br^- and TiO_6^{2-} octahedron.

3.5 Photocatalytic activity of TiO_2

Fig.7 showed the degradation results of reactive brilliant blue KN-R under UV irradiation by the P25, Sample A and B. It was observed that the TiO_2 prepared with IL, the Sample B, showed the highest adsorption and degradation capacity among them.

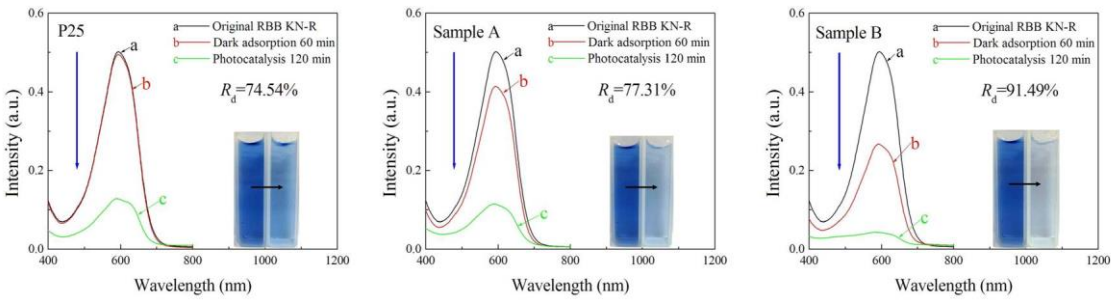

Fig.7 Photo-catalytic degradation of RBB by the P25, Sample A and B

And, it was more obvious that the adsorption quantity of Sample B was the most among them. The reason was that the TiO_2 prepared with IL were synthesized at low temperature and ambient pressure, without high-temperature calcinations, had more uniform vesicular structure and higher specific surface area. So the molecular of RBB not only can adsorped the surface of TiO_2 particles, but also across the porous structure. All of these offered conditions to the photocatalysis, so the Sample B showed the highest photocatalytic capacity, the degradation percent of the RBB by Sample (b) for 2 hours with UV mercury lamp was 91.49%. The clear progress of photocatalysis was showed in Fig.8.

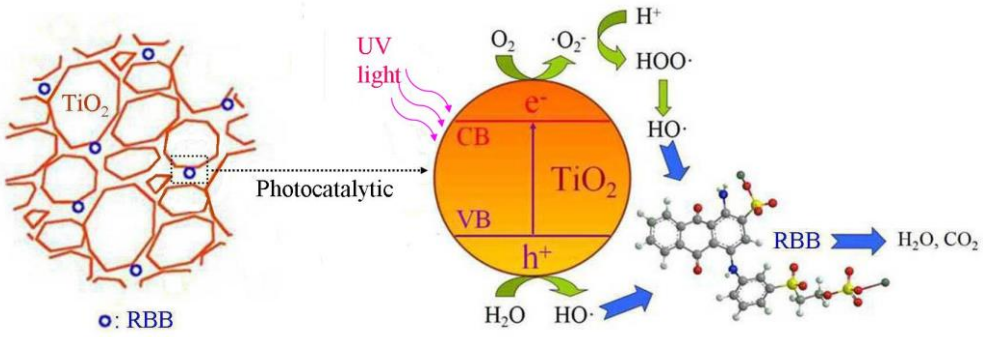

Fig.8 Schematic of the photodegradation in the microspheres of Sample B

As the Fig.8 showed that the reactive brilliant blue was not only adsorbed largely on the surface of TiO_2 because of higher specific surface area, but also could enter into the inter-space of vesicular structure and contacted TiO_2 particles directly, just like the describe in the left of the picture. Meanwhile, uniform vesicular structure with big specific pore volume offered convenience to TiO_2 which adsorbed and used dissolved oxygen in water. As the right of the picture seen, when TiO_2 were shined by UV mercury lamp, TiO_2 can produced electrons and they jumped from valence band to conduct band, so photo-generated hole(h^+) and photo-generated electron(e^-) formed. O_2 and H_2O in the liquid can finally produce HO· through the combine with photo-generated electron(e^-). It owned strong oxidability, it can degrade reactive brilliant blue into H_2O and CO_2 [22, 23]. All of these maked the TiO_2 prepared with IL prove better photo-catalytic activity than P25.

4. Conclusions

Porous anatase TiO_2 with high surface area and uniform pore structure has been synthesized at 60℃ and ambient pressure by using [C_6mim]Br. The [C_6mim]Br is an effective template to assisted the preparation of TiO_2 by sol-gel method. It enhances the polycondensation and crystallization rate, which encourages the formation of anatase crystal. In addition, the TiO_2 prepared with IL exhibits better photocatalytic activity than P25.

Acknowledgments

This work is financially supported by National Natural Science Foundation of China (No. 21106011, 21276034, 21243005).

References

[1] H. Liu, Y.G.. Liang, H.J. Hu, M.Y. Wang. Solid. State. Sci. **11**, 1655 (2009)

[2] Z.Y. Yan, Q. Liu, W.J. Zheng, Chinese. J. Inorg. Chem. **22**, 2055 (2006)
[3] Twerek A, Alexander B, Osama S, Anja VM. Mater. Chem. Phys. **120**, 109 (2010)
[4] J.G. Yu, Q. Li, S.W. Liu, M. Jaroniec, Chem. Eur. J. **19**, 2433 (2013)
[5] W.J. Zheng, X.D. Liu, Z.Y. Yan, L.J. Z, ACS. Nano. **3**, 115 (2009)
[6] K. S. Yoo, H. Choi, D. Dionysion, Chem. Commun. **17**, 2000 (2004)
[7] K. S. Yoo, H. Choi, D. Dionysiou, Catal. Commun. **6**, 259 (2005)
[8] H. Yin, Y. Wada, T. Kitamura, et al. J. Mater. Chem. **11**, 1694 (2001)
[9] Y. Zhou, H. J. Schattka, M. Antonietti, Nano Lett **4**, 477 (2004)
[10] H. Zhang , M. Finnegan, J.F. Ban field, Nano Lett. **1**, 81 (2001)
[11] J. Overstone , K. Yanagisawa, Chem. Mater. **11**, 2770 (1999)
[12] H.C. Eun, H. Suk-In, M.J. Dong, Catal. Lett. **123**, 84 (2008)
[13] Y. Liu, J. Li, M.J. Wang, Z.Y. Li, H.T. Liu, P. He, X.R. Yang, J.H. Li, Cryst. Growth. Des. **5**, 1643 (2005)
[14] T.A. Kandiel, A.A. Ismail, D.W. Bahnemann, Phys. Chem. Chem. Phys. **13**, 20155 (2011)
[15] S.T. Aruna, S. Tirosh , A. Zaban, J. Mater. Chem. **10**, 2388 (2000)
[16] Z.Q. Zhao, X.L. Jiao, D.R. Chen, J. Mater. Chem. **19**, 3078 (2009)
[17] S. Liu, N. Jaffrezic, C. Guillard, Appl. Surf. Sci. **255**, 2704 (2008)
[18] M.C. Yan, F. Chen, J.L. Zhang, M. Anpo, J. Phys. Chem. B **109**, 8673 (2005)
[19] J.S. Beck, J.C. Vartuli, W.J. Roth, M.E. Leonowicz, C.T. Kresge, K.D. Schmitt, C.T.W. Chu, D.H. Olson, E.W. Sheppard, J. Am. Chem. Soc. **114**, 10834 (1992)
[20] C.T. Kresge, M.E. Leonowicz, Nature **359**, 710 (1992)
[21] S. Li, D. Zhao, J. Zheng, X. Xue, H. Sun, H. Sun, C. Shen, J. Porous Mater. **20**, 473 (2013)
[22] T. Nakashima, N. Kimizuka, J. Am. Chem. Soc. **125**, 6386 (2003)
[23] H.L. Zhang, C.J. Tang, Y.Y. Lv, F. Gao, L. Dong, J. Porous Mater. **21**, 63 (2014)